Hindawi Publishing Corporation
Journal of Nanomaterials
Volume 2014, Article ID 710874, 6 pages
http://dx.doi.org/10.1155/2014/710874

Research Article

Fabrication of Novel 2D NiO Nanosheet Branched on 1D-ZnO Nanorod Arrays for Gas Sensor Application

Le Thuy Hoa, Huynh Ngoc Tien, and Seung Hyun Hur

School of Chemical Engineering and Bioengineering, University of Ulsan, Daehak-ro 102, Nam-gu, Ulsan 680-749, Republic of Korea

Correspondence should be addressed to Seung Hyun Hur; shhur@ulsan.ac.kr

Received 4 August 2014; Revised 27 October 2014; Accepted 28 October 2014; Published 13 November 2014

Academic Editor: Santanu K. Maiti

Fabrication of 3D structures composed of 1D n-type ZnO nanorods (NRs) and 2D p-type NiO nanosheets (NSs) by a low-cost, low-temperature, and large-area scalable hydrothermal process and its use in highly sensitive NO_2 gas sensors were studied. The p-n heterojunctions formed by NiO-ZnO interfaces as well as large area two-dimensional NiO NSs themselves increased the adsorption of NO_2. Moreover, the charge transfer between NiO and ZnO enhanced the responsivity and sensitivity of NO_2 sensing even at a concentration of 1 ppm. The 30-min NiO NS growth on ZnO NRs in the hybrid sensor showed the highest sensitivity due to the formation of optimum p-n heterojunctions between ZnO NRs and NiO NSs for gas adsorption and carrier transport. Low responsivity toward reducing gases was also observed.

1. Introduction

Among various metal oxide semiconductors, zinc oxide (ZnO) has been used extensively due to its beneficial electrical properties such as wide band gap (3.37 eV) and large binding energy (60 meV). When hybridized with other materials, ZnO showed unique properties that can be used effectively for many types of electronic devices including gas sensors [1, 2], solar cells [3, 4], and UV sensors [5, 6]. Moreover, it can be easily grown by hydrothermal methods in the form of nanostructures such as nanorods and nanowires that can exhibit enhanced properties due to increased surface area to volume ratios. Due to its excellent resistance to various chemicals, nickel oxide (NiO) has been widely explored for gas sensors [7, 8], supercapacitors [9, 10], electrochromic devices [11, 12], and lithium ion batteries [13, 14]. A wide range of NiO nanostructures, such as thin films [15, 16], nanotubes [17, 18], and flake-like structures [19], can be formed by sputtering methods [20, 21], sol-gel processes [22, 23], and hydrothermal synthesis [24, 25]. Recent studies also demonstrated that the hybrid structures composed of NiO nanotubes and ZnO shells exhibited highly improved hydrogen sulfide (H_2S) sensing properties by the formation of heterointerfaces [26]. In our previous work we showed that optimized hybrid structures of NiO and ZnO can be effectively used as optical sensors due to improved charge transfer and decreased recombination of excitons.

In this paper, the 3D hybrid structures composed of n-type 1D ZnO nanorods (NRs) and p-type 2D NiO nanosheets (NSs) with different NiO growth times were fabricated using low-cost and easy hydrothermal methods (Figure 7). These were used to detect toxic gas, such as nitrogen oxide (NO_2), which has a characteristic sharp, biting odor and is regarded as a prominent air pollutant. Due to the charge transfer between the two nanostructures as well as increased adsorption sites formed by large-area 2D NiO NSs and electron-depleted p-n junctions, the NiO NS/ZnO NR hybrid structures exhibited improved NO_2 sensing properties. At optimized conditions, the hybrid structures showed a 2800-fold higher sensitivity than pure ZnO NRs and pure NiO NSs, even at very low NO_2 concentrations (1 ppm). They also exhibited good selectivity toward NO_2 when other gases, including H_2, NH_3, and H_2S, were tested and compared.

2. Experimental

The hybrid structure was fabricated step by step as described in our previous study [27].

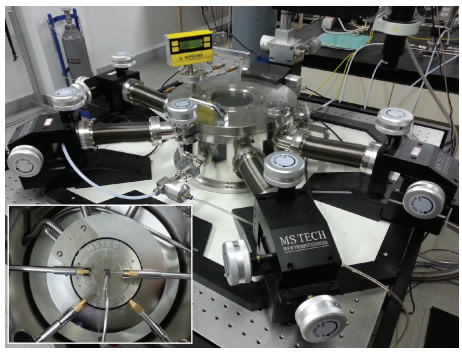

Figure 1: The MST-5000 gas sensor system (MST-5000, MS-Tech) and the chamber equipped with a heating plate and probes (inset), gas flow was controlled precisely by mass flow controllers, and nitrogen was used as a carrier gas.

2.1. Growth of ZnO NRs. The primary step is growing vertically aligned ZnO NRs on the sensing electrode via a hydrothermal process. In brief, diethanolamine ($HN(CH_2CH_2OH)_2$, Sigma-Aldrich) was added slowly into the mixed solution, which was composed of zinc acetate dehydrate ($Zn(CH_3COO)_2{\cdot}2H_2O$ 98%, Sigma-Aldrich) and 2-methoxyethanol ($CH_3OC_2H_5OH$, Sigma-Aldrich), under continuous magnetic stirring at 70°C for 2 h. Then, the solution was spin-coated onto the sensing electrode patterned SiO_2/Si wafer and annealed in air at 400°C for 4 h. ZnO NRs were grown by exposing the prepared seed layer to the mixed aqueous solution of zinc nitrate hexahydrate 0.02 M ($Zn(NO_3)_2{\cdot}6H_2O$, Sigma-Aldrich) and hexamethylenetetramine 0.02 M ($C_6H_{12}N_4$, Sigma-Aldrich) at 90°C for 5 h. ZnO NRs were rinsed with deionized water several times and dried in a vacuum oven before the next steps.

2.2. Growth of NiO NSs. To grow NiO NSs on the ZnO NR surface, the Ni seed solution was first prepared by mixing nickel acetate tetrahydrate ($Ni(OCOCH_3)_2{\cdot}4H_2O$, Sigma-Aldrich) with 2-methoxyethanol ($CH_3OCH_2CH_2OH$, Sigma-Aldrich) and diethanolamine ($HN(CH_2CH_2OH)_2$, Sigma-Aldrich) under continuous magnetic stirring at 70°C for 2 h. Then, the mixed solution was spin-coated onto the ZnO NRs and annealed in air at 400°C for 4 h to form a Ni seed layer. Next, the ZnO NRs covered with the Ni seed layer were directly exposed to a mixed aqueous solution of nickel nitrate hexahydrate 0.02 M ($Ni(NO_3)_2{\cdot}6H_2O$ 98%, Sigma-Aldrich) and hexamethylenetetramine 0.02 M ($C_6H_{12}N_4$, Sigma-Aldrich) at 90°C to grow NiO NSs. Finally, NiO NSs/ZnO NRs were rinsed and annealed in air at 400°C for 4 h.

2.3. Instrumental Analysis. The structures of NiO NSs/ZnO NRs, NiO NSs, and ZnO NRs were characterized by X-ray diffraction (XRD) and field-emission scanning electron microscopy (FE-SEM) after thin film growth on the SiO_2/Si wafer. Gas sensing properties were measured using a MST-5000 chamber (MS-Tech, Figure 1) at 200°C. Gas flow was precisely controlled using a mass flow controller (GMC 1200, ATOVAC) and nitrogen (N_2) was used as a carrier gas. A semiconductor parameter analyzer (Hewlett-Packard-4155A) was used to measure the resistance of sensing devices.

3. Results and Discussion

The morphology change of NiO NSs on the ZnO NRs at different NiO growth times was investigated and is shown in Figure 2. We can only infer the growth of NiO NSs by the increased roughness of ZnO NRs or some fibril-like structures between ZnO NRs at short growth times (Figures 2(a) and 2(b)). Instead, the 3D networks of NiO NSs between ZnO NRs are clearly observed after longer growth times, which implies that various morphologies of NiO NS/ZnO NR hybrid structures that have different Ni/Zn ratios can be realized by changing the NiO growth time.

In order to verify the crystal structure and phase purity of the samples, XRD analysis was used, and these results are shown in Figure 3. NiO NSs exhibit three characteristic peaks at 37.30°, 43.28°, and 65.23°, which, respectively, correspond to the (111), (200), and (220) planes of bunsenite structure NiO [28]. ZnO NR shows peaks at 31.87°, 34.54°, 56.81°, and 67.23°, which, respectively, correspond to the (100), (002), (110), and (201) planes of hexagonal structure of ZnO [29]. The intensity ratio of $I_{Ni(220)}/I_{Zn(002)}$ was increased from 0.2538 to 4.4134 as the NiO growth time increased from 5 min to 60 min, which indicates continuous growth of NiO NSs on the ZnO NRs.

The atomic composition and TEM image were shown in Figure 4. Both the Zn and Ni atoms were observed in the energy dispersive X-ray (EDX) analysis and ZnO NR covered with NiO NS was also clearly observed in the TEM image.

The *I-V* characteristics of ZnO NRs, NiO NSs, and NiO NSs/ZnO NRs were measured to investigate the electrical resistance of each sample. The electrodes used in this study were prepared following our previous study [27]. As shown in Figure 5, after decorating the NiO NSs with ZnO NRs, the conductance was decreased due to the formation of local electron depletion layers at the heterojunctions between p-type NiO and n-type ZnO. The electrical resistivity of ZnO nanorods calculated using the thickness of the ZnO seed layer, as shown in the inset of Figure 4, was approximately 4.14×10^{-5} Ω·cm, which was higher than that of a previous report because hydrothermal synthesis was used in this study [28].

NO_2 responsivity (RS, $(R_g - R_a)/R_g$ (%)) and sensitivity (RS/gas concentration (ppm)) of the NiO NSs/ZnO NRs and NiO NSs alone were measured at low levels of NO_2, where R_a and R_g are the resistances of the sensing layer measured in the atmosphere of only N_2 and NO_2/N_2 gas mixture, respectively. As shown in Figure 6, the NiO NS/ZnO NR hybrid structure exhibited around a 6-fold higher responsivity and 9-fold higher sensitivity than those of NiO NSs, which has a large enough adsorption area. The sensitivity obtained in this study of 3.4026 ppm^{-1} from the NiO NS (30 min growth time)/ZnO NR sample is three orders (~2800-fold) higher than that of pure ZnO NRs and even one order (~20-fold) higher than that of 0-D CuO nanoparticles decorated with 1D ZnO NR

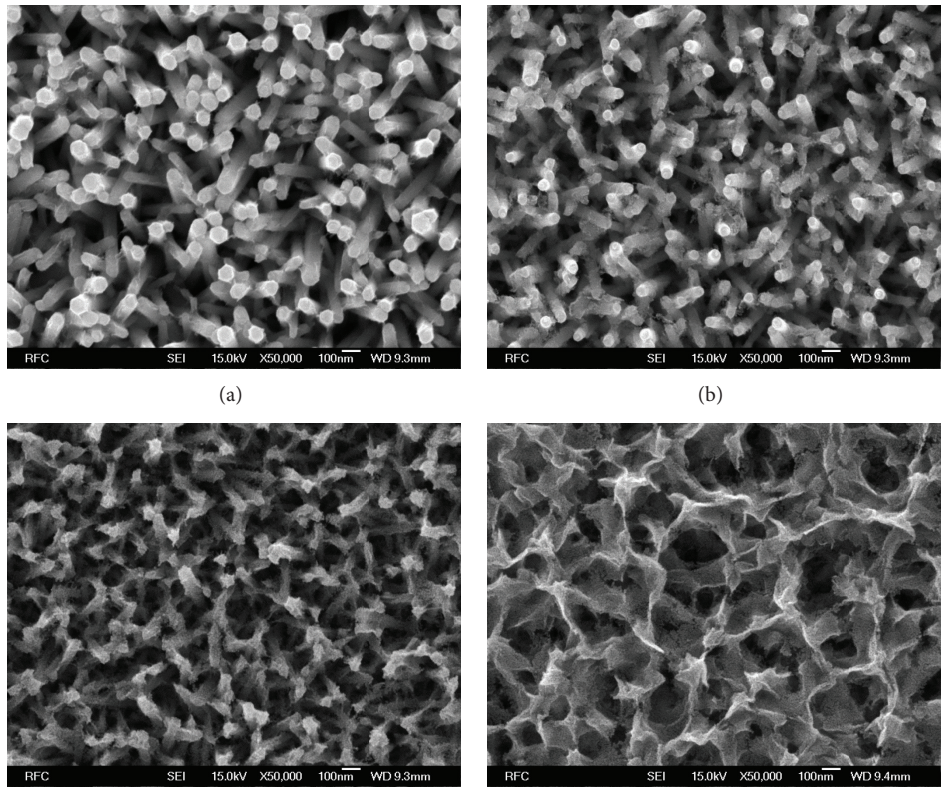

Figure 2: SEM images of NiO NSs grown on ZnO NRs for (a) 5 min, (b) 15 min, (c) 45 min, and (d) 60 min.

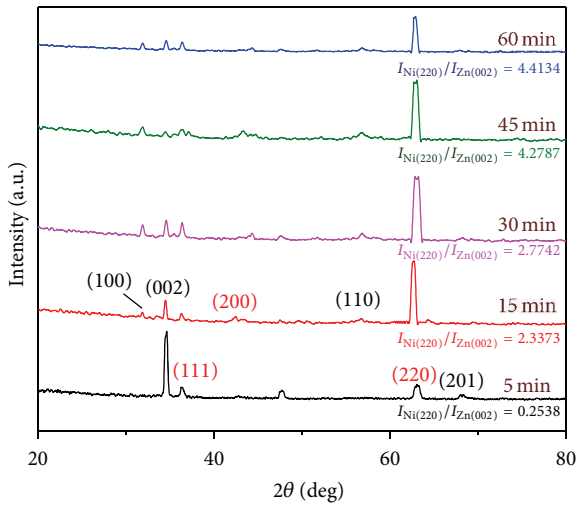

Figure 3: XRD spectra of NiO NSs grown on ZnO NRs at various NiO NS growth times from 5 min to 60 min.

that were reported previously [29]. The fast response time of NiO NS/ZnO NR than that of NiO NS was observed, which can be due to the high amount of p-n junction sites that can effectively adsorb NO_2 molecules. It is also interesting to note that the NO_2 sensitivity increased initially as the NiO NS growth time increased until 30 min then the NO_2 sensitivity decreased gradually, which indicates the presence of an optimum ratio of NiO NSs and ZnO NRs. In turn, excess growth of NiO NSs will cover the whole ZnO NR surface and thus synergetic effects between NiO NSs and ZnO NRs cannot be expected.

The improved NO_2 response and sensitivity of the NiO NS/ZnO NR hybrid structure can be explained as follows. First, increased surface area after NiO NS growth on ZnO provided a larger NO_2 adsorption area. In addition, the numerous electron-depletion layers that formed at the p-NiO NS and n-ZnO heterojunction region attracted the gases more than bare ZnO NRs or NiO NSs alone, which results in more NO_2 adsorption even at low concentration [30]. Another important fact is the charge transfer between p-type NiO NSs and n-type ZnO NRs [28]. When NO_2 gas is exposed to the NiO NSs, the NO_2 first reacts with the adsorbed O^- ions on NiO as NO_2 has higher electron affinity than that of the preadsorbed oxygen [31]; this results in the generation of holes on NiO surfaces:

$$NO_2\,(\text{gas}) \longrightarrow NO_2\,(\text{ads}) \quad (1)$$

$$NO_2\,(\text{ads}) \longrightarrow NO_2^-\,(\text{ads}) + h^+ \quad (2)$$

Then, the transfer of holes from p-type NiO to n-type ZnO (loss of electrons of n-type ZnO) leads to a resistance increase of the ZnO seed layer that carries charges between two electrodes. Without NiO-ZnO heterojunctions (NiO

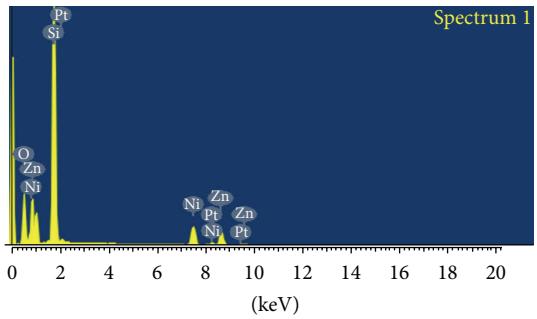

(a)

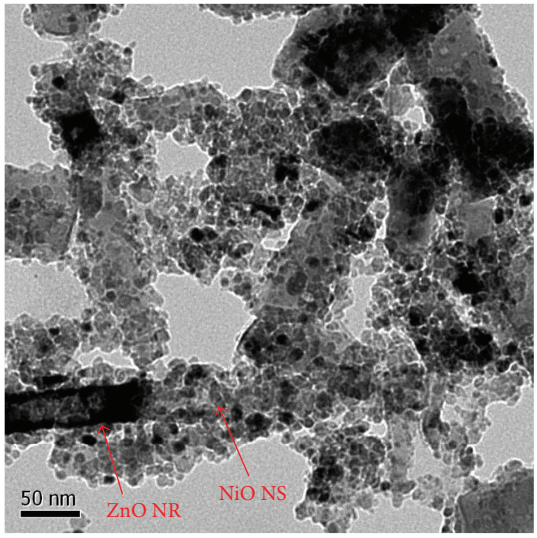

(b)

Figure 4: (a) EDX spectrum of NiO NSs/ZnO NRs and (b) TEM image of ZnO NR covered with NiO NS.

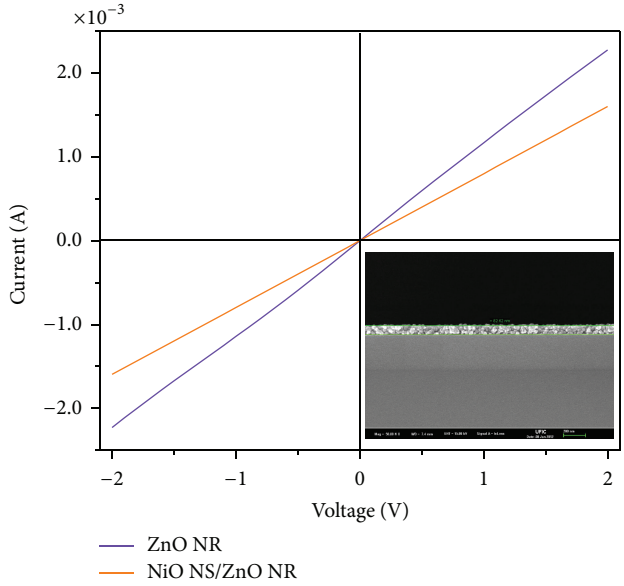

Figure 5: *I-V* curves of ZnO NRs and NiO NSs/ZnO NRs. The inset shows a cross-sectional SEM image of ZnO seed layer.

alone), there will be hole accumulation on the NiO surface, which will cause low responsivity due to the suppressed further adsorption of NO_2. On the other hand, in the presence of p-n heterojunctions, hole transfer from NiO NSs to ZnO NRs will prevent the accumulation of holes in NiO NSs, thus maintaining the adsorption of NO_2. This will enhance both the responsivity and sensitivity of sensing layers.

The responsivity of fabricated NiO NS/ZnO NR gas sensors toward reducing gases, such as H_2S, H_2, and NH_3, was also investigated. As shown in Figure 6, the responsivity for reducing gases was lower than that for NO_2 gas, which can be due to the low catalytic effect during the adsorption of reducing gases [32]. As described in the following reaction, when reducing gases are adsorbed onto the metal oxide surface they are oxidized through the reaction with preadsorbed oxygen ions. Due to the low dissociative chemisorption of hydrogen by the NiO, there is less electron generation, which results in the lower responsivity of NiO NS/ZnO NR sensors for reducing gases than that for NO_2. The surface modification by Pt, which has excellent H_2 adsorption and catalytic dissociation ability, can enhance the responsivity of NiO-based sensors toward reducing gases [33]:

$$H_2\,(\text{gas}) + O^-\,(\text{ads}) \longrightarrow H_2O + e^- \qquad (3)$$

The highest responsivity at 30 min of NiO NS growth indicates the similar synergetic effect of charge transfer between NiO NSs and ZnO NRs as the NO_2 gas case. The negative responsivity of the hybrid sensor for reducing gases is due to the electron generated by the oxidation of reducing gases. Electrons transferred from the p-type NiO NSs to n-type ZnO might decrease the resistance of n-type ZnO, which acts as channel materials for carrier transport in the sensing devices.

4. Conclusions

The 3D structures composed of 1D ZnO NRs and 2D NiO NSs were fabricated by an easy and cost-effective hydrothermal synthesis method, and these were then used for NO_2 sensors. Due to the increased surface areas, formation of electron depletion layers at ZnO-NiO heterojunctions, and effective carrier transport between two nanostructured semiconductors, the NiO NS/ZnO NR sensors exhibited highly improved sensitivity toward NO_2 gases over pure NiO NS and ZnO NR sensors. It was also observed that at a 30 min NiO NS growth on ZnO NRs, hybrid sensors exhibited maximum NO_2 sensitivity due to the formation of optimized 1D-2D p-n heterojunction hybrid structures. Due to the low dissociative chemisorption of H_2 on NiO, hybrid sensors exhibited low response toward reducing gases, which results in improved selectivity. We think that this type of 3D structures can be effectively used in many gas-sensing applications due to its simple fabrication process and high sensing performance.

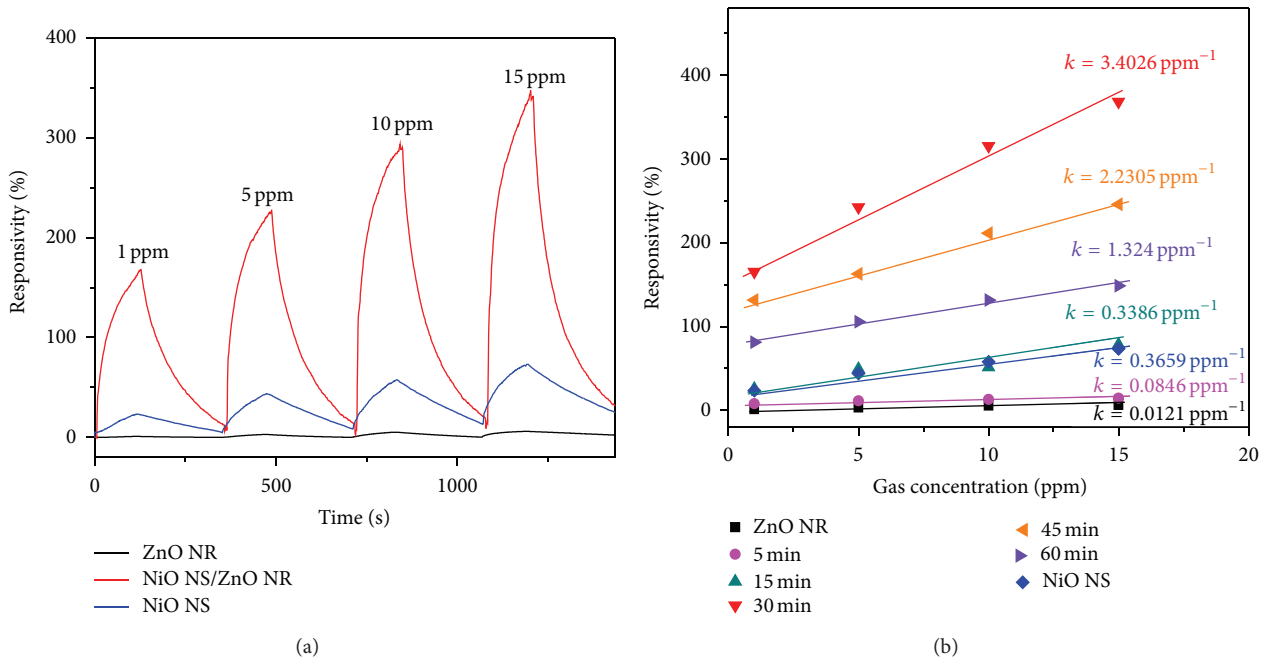

FIGURE 6: (a) Responsivity of pure NiO NSs and NiO NSs/ZnO NRs at 30 min NiO growth and (b) the sensitivity of NiO NSs/ZnO NRs at various NiO growth times toward various NO_2 gas concentrations.

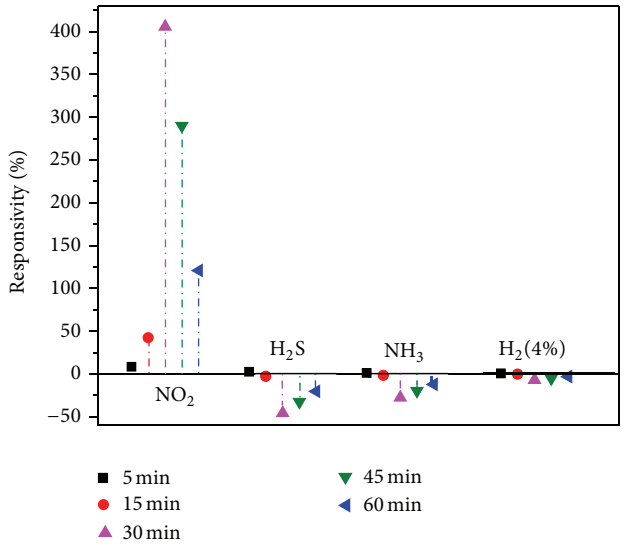

FIGURE 7: Responsivity of NiO NS/ZnO NR sensors at different NiO growth times under various gases. Concentrations of NO_2, H_2S, and NH_3 were 100 ppm and that of H_2 was 4%, respectively.

Conflict of Interests

All authors have no conflict of interests to declare. This statement is to certify that all authors have seen and approved the paper being submitted. The authors warrant that the paper is the authors' original work. The authors warrant that the paper has not received prior publication and is not under consideration for publication elsewhere. On behalf of all coauthors, the corresponding author shall bear full responsibility for the submission. This research has not been submitted for publication nor has it been published in whole or in part elsewhere.

Acknowledgment

This research was supported by the Basic Science Research Program through the National Research Foundation of Korea (NRF) funded by the Ministry of Education (2013R1A1A2A10004468).

References

[1] Q. Wan, Q. H. Li, Y. J. Chen et al., "Fabrication and ethanol sensing characteristics of ZnO nanowire gas sensors," *Applied Physics Letters*, vol. 84, no. 18, pp. 3654–3656, 2004.

[2] M.-W. Ahn, K.-S. Park, J.-H. Heo et al., "Gas sensing properties of defect-controlled ZnO-nanowire gas sensor," *Applied Physics Letters*, vol. 93, no. 26, Article ID 263103, 2008.

[3] S. H. Ko, D. Lee, H. W. Kang et al., "Nanoforest of hydrothermally grown hierarchical ZnO nanowires for a high efficiency dye-sensitized solar cell," *Nano Letters*, vol. 11, no. 2, pp. 666–671, 2011.

[4] K. Matsubara, P. Fons, K. Iwata et al., "ZnO transparent conducting films deposited by pulsed laser deposition for solar cell applications," *Thin Solid Films*, vol. 431-432, pp. 369–372, 2003.

[5] H. Ohta, M. Kamiya, T. Kamiya, M. Hirano, and H. Hosono, "UV-detector based on pn-heterojunction diode composed of transparent oxide semiconductors, p-NiO/n-ZnO," *Thin Solid Films*, vol. 445, no. 2, pp. 317–321, 2003.

[6] C. S. Lao, M.-C. Park, Q. Kuang et al., "Giant enhancement in UV response of ZnO nanobelts by polymer surface-functionalization," *Journal of the American Chemical Society*, vol. 129, no. 40, pp. 12096–12097, 2007.

[7] I. Hotovy, V. Rehacek, P. Siciliano, S. Capone, and L. Spiess, "Sensing characteristics of NiO thin films as NO_2 gas sensor," *Thin Solid Films*, vol. 418, no. 1, pp. 9–15, 2002.

[8] H. Steinebach, S. Kannan, L. Rieth, and F. Solzbacher, "H_2 gas sensor performance of NiO at high temperatures in gas mixtures," *Sensors and Actuators B: Chemical*, vol. 151, no. 1, pp. 162–168, 2010.

[9] J. W. Lee, T. Ahn, J. H. Kim, J. M. Ko, and J.-D. Kim, "Nanosheets based mesoporous NiO microspherical structures via facile and template-free method for high performance supercapacitors," *Electrochimica Acta*, vol. 56, no. 13, pp. 4849–4857, 2011.

[10] J. Cheng, G.-P. Cao, and Y.-S. Yang, "Characterization of sol-gel-derived NiO_x xerogels as supercapacitors," *Journal of Power Sources*, vol. 159, no. 1, pp. 734–741, 2006.

[11] X. H. Xia, J. P. Tu, J. Zhang, X. L. Wang, W. K. Zhang, and H. Huang, "Electrochromic properties of porous NiO thin films prepared by a chemical bath deposition," *Solar Energy Materials & Solar Cells*, vol. 92, no. 6, pp. 628–633, 2008.

[12] Z. Jiao, M. Wu, Z. Qin, and H. Xu, "The electrochromic characteristics of sol-gel-prepared NiO thin film," *Nanotechnology*, vol. 14, no. 4, pp. 458–461, 2003.

[13] B. Varghese, M. V. Reddy, Z. Yanwu et al., "Fabrication of NiO nanowall electrodes for high performance lithium ion battery," *Chemistry of Materials*, vol. 20, no. 10, pp. 3360–3367, 2008.

[14] S. A. Needham, G. X. Wang, and H. K. Liu, "Synthesis of NiO nanotubes for use as negative electrodes in lithium ion batteries," *Journal of Power Sources*, vol. 159, no. 1, pp. 254–257, 2006.

[15] K.-W. Nam, W.-S. Yoon, and K.-B. Kim, "X-ray absorption spectroscopy studies of nickel oxide thin film electrodes for supercapacitors," *Electrochimica Acta*, vol. 47, no. 19, pp. 3201–3209, 2002.

[16] P. S. Patil and L. D. Kadam, "Preparation and characterization of spray pyrolyzed nickel oxide (NiO) thin films," *Applied Surface Science*, vol. 199, no. 1–4, pp. 211–221, 2002.

[17] G. Malandrino, L. M. S. Perdicaro, I. L. Fragalà, R. L. Nigro, M. Losurdo, and G. Bruno, "MOCVD template approach to the fabrication of free-standing nickel(II) oxide nanotube arrays: structural, morphological, and optical properties characterization," *The Journal of Physical Chemistry C*, vol. 111, no. 8, pp. 3211–3215, 2007.

[18] H. Pang, Q. Lu, Y. Li, and F. Gao, "Facile synthesis of nickel oxide nanotubes and their antibacterial, electrochemical and magnetic properties," *Chemical Communications*, no. 48, pp. 7542–7544, 2009.

[19] J.-W. Lang, L.-B. Kong, W.-J. Wu, Y.-C. Luo, and L. Kang, "Facile approach to prepare loose-packed NiO nano-flakes materials for supercapacitors," *Chemical Communications*, no. 35, pp. 4213–4215, 2008.

[20] H.-L. Chen, Y.-M. Lu, and W.-S. Hwang, "Characterization of sputtered NiO thin films," *Surface and Coatings Technology*, vol. 198, no. 1–3, pp. 138–142, 2005.

[21] Y. M. Lu, W. S. Hwang, and J. S. Yang, "Effects of substrate temperature on the resistivity of non-stoichiometric sputtered NiO_x films," *Surface and Coatings Technology*, vol. 155, no. 2-3, pp. 231–235, 2002.

[22] J. L. Garcia-Miquel, Q. Zhang, S. J. Allen et al., "Nickel oxide sol-gel films from nickel diacetate for electrochromic applications," *Thin Solid Films*, vol. 424, no. 2, pp. 165–170, 2003.

[23] E. O. Zayim, I. Turhan, F. Z. Tepehan, and N. Ozer, "Sol-gel deposited nickel oxide films for electrochromic applications," *Solar Energy Materials & Solar Cells*, vol. 92, no. 2, pp. 164–169, 2008.

[24] D.-B. Kuang, B.-X. Lei, Y.-P. Pan, X.-Y. Yu, and C.-Y. Su, "Fabrication of novel hierarchical β-$Ni(OH)_2$ and NiO microspheres via an easy hydrothermal process," *The Journal of Physical Chemistry C*, vol. 113, no. 14, pp. 5508–5513, 2009.

[25] L. Wang, Y. Hao, Y. Zhao, Q. Lai, and X. Xu, "Hydrothermal synthesis and electrochemical performance of NiO microspheres with different nanoscale building blocks," *Journal of Solid State Chemistry*, vol. 183, no. 11, pp. 2576–2581, 2010.

[26] L. Xu, R. Zheng, S. Liu et al., "NiO@ZnO heterostructured nanotubes: coelectrospinning fabrication, characterization, and highly enhanced gas sensing properties," *Inorganic Chemistry*, vol. 51, no. 14, pp. 7733–7740, 2012.

[27] L. T. Hoa, H. N. Tien, and S. H. Hur, "A highly sensitive UV sensor composed of 2D NiO nanosheets and 1D ZnO nanorods fabricated by a hydrothermal process," *Sensors and Actuators A: Physical*, vol. 207, pp. 20–24, 2014.

[28] L. T. Hoa, H. N. Tien, V. H. Luan, J. S. Chung, and S. H. Hur, "Fabrication of a novel 2D-graphene/2D-NiO nanosheet-based hybrid nanostructure and its use in highly sensitive NO_2 sensors," *Sensors and Actuators B: Chemical*, vol. 185, pp. 701–705, 2013.

[29] L. T. Hoa and S. H. Hur, "Highly sensitive NO_2 sensors based on local p–n heterojunctions composed of 0D CuO nanoparticles and 1D ZnO nanorods," *Physica Status Solidi (A)*, vol. 210, no. 6, pp. 1213–1216, 2013.

[30] C. W. Na, H.-S. Woo, I.-D. Kim, and J.-H. Lee, "Selective detection of NO_2 and C_2H_5OH using a Co_3O_4-decorated ZnO nanowire network sensor," *Chemical Communications*, vol. 47, no. 18, pp. 5148–5150, 2011.

[31] N. D. Hoa and S. A. El-Safty, "Synthesis of mesoporous NiO nanosheets for the detection of toxic NO_2 gas," *Chemistry*, vol. 17, no. 46, pp. 12896–12901, 2011.

[32] A. Borgschulte, R. J. Westerwaal, J. H. Rector, B. Dam, and R. Griessen, "Hydrogen sorption mechanism of oxidized nickel clusters," *Applied Physics Letters*, vol. 85, no. 21, pp. 4884–4886, 2004.

[33] I. Hotovy, J. Huran, P. Siciliano, S. Capone, L. Spiess, and V. Rehacek, "Enhancement of H_2 sensing properties of NiO-based thin films with a Pt surface modification," *Sensors and Actuators B: Chemical*, vol. 103, no. 1-2, pp. 300–311, 2004.